Human With No Lysine Kinase 3 (WNK3)

A Target Enabling Package (TEP)

Gene ID / UniProt ID / EC	WNK3, 65267 / Q9BYP7 / E.C. 2.7.11.1.
Target Nominator	Dario Alessi (University of Dundee, UK)
SGC Authors	Daniel M Pinkas, Joshua C Bufton, Sergio G. Bartual, Zhuoyao Chen, Fiona J Sorrell, Alex N Bullock
Collaborating Authors	Gerrit M. Daubner[1], Frances-Rose Schumacher[1], George Georghiou[2], Jinwei Zhang[1], Thimo Kurz[3], Dario R Alessi[1]
Target PI	Alex Bullock (SGC Oxford)
Therapeutic Area(s)	Metabolic diseases
Disease Relevance	WNK3 is linked to hypertension and its knockout improves neurological recovery after stroke
Date approved by TEP Evaluation Group	2nd June 2017
Document version	Version 4
Document version date	June 2018
Citation	Daniel M Pinkas, Joshua C Bufton, Sergio G. Bartual, Zhuoyao Chen, Gerrit M. Daubner, Frances-Rose Schumacher, George Georghiou, Jinwei Zhang, Fiona J Sorrell, Thimo Kurz, Dario R Alessi, and Alex N Bullock (2017) Human With No Lysine Kinase 3 (WNK3); A Target Enabling Package. 10.5281/zenodo.1219718.
Affiliations	1. College of Life Sciences, University of Dundee 2. European Bioinformatics Institute (EMBL-EBI) 3. Institute of Molecular Cell and Systems Biology, University of Glasgow

We respectfully request that this document is cited using the DOI reference as given above if the content is used in your work.

USEFUL LINKS

GeneCards HUMAN GENE DATABASE | Open Targets | 50 YEARS OMIM Human Genetics Knowledge for the World | IMPC International Mouse Phenotyping Consortium | ChEMBL

(Please note that the inclusion of links to external sites should not be taken as an endorsement of that site by the SGC in any way)

SUMMARY OF PROJECT

Kinases WNK1-4 regulate cation-chloride cotransporters via phosphorylation of SPAK and OSR1 and thereby control salt homeostasis, cell volume and blood pressure. Gain of function mutations in WNK kinases are found in Gordon's hypertension syndrome suggesting the WNK pathway as a therapeutic target. WNK3 inhibition in particular has also been shown to reduce cerebral injury after Ischemic stroke. Here we present assays and crystal structures that define (i) the molecular basis for disease mutations; (ii) the multiple functional domains of WNK kinases and their protein interactions; (iii) the binding of small molecule kinase inhibitors and a potential allosteric pocket.

SCIENTIFIC BACKGROUND

WNK1-4 (with no lysine) are chloride-sensing kinases with an atypical β2-strand catalytic lysine instead of β3. They phosphorylate kinases SPAK and OSR1 which in turn mediate regulatory phosphorylations on cation-chloride cotransporters (e.g. NKCC1, NKCC2, NCC)(**Fig.1**).

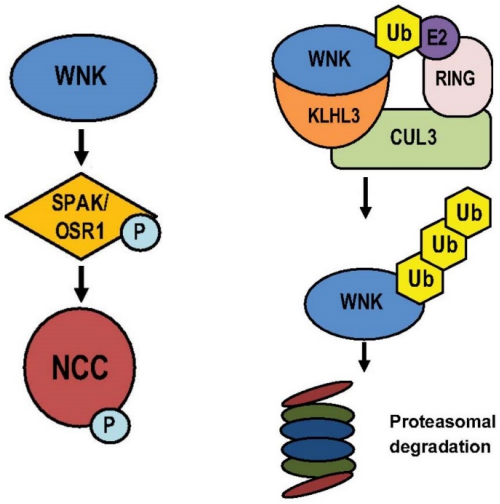

Fig.1. Schematic representation of WNK signalling and regulation by the ubiquitin-proteasome system (adapted from Am J Physiol Renal Physiol 2016; 310(11), F1389-96.)

RFXV motifs in WNKs and co-transporters mediate interactions with Conserved C-Terminal (CCT) domains in SPAK, OSR1 and WNK1-4. WNKs can also dimerise through a coiled-coil domain and contain a degron motif for ubiquitin-dependent degradation by the E3 KLHL3/CUL3 (**Fig. 2**)

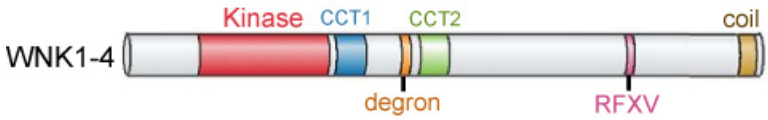

Fig. 2. General domain organisation of WNK kinases.

WNK1 and WNK4 are expressed in the kidney where they regulate salt homeostasis, cell volume and blood pressure. WNK isoforms including WNK3 are also expressed in the brain where their control of salt homeostasis regulates GABAergic signalling.
Mutations in the degron motifs of WNK1 or WNK4 or the E3 ligase KLHL3-CUL3 block WNK degradation causing a gain of function in Gordon's Syndrome (also known as pseudohypoaldosteronism type II), a rare familial autosomal dominant disease leading to severe hypertension (1). Polymorphisms in WNK3 also link to hypertension in the Chinese population (2).
Gain of function mutations in WNK kinases in hypertension suggest an application for WNK pathway inhibitors. Ischemia has also been shown to induce aberrant NKCC1 activation, cell death and cerebral injury after stroke. WNK3 knockout in mice reduced the associated brain damage and improved neurological recovery (3).

RESULTS – THE TEP

Proteins purified

KLHL3 kelch domain (used for crystallography, assays)
Human KLHL3 kelch domain (a.a. 298–587) was cloned into pNIC28-Bsa4, expressed in BL21(DE3)-R3-pRARE cells and purified using Ni-affinity, ion exchange and size exclusion chromatography.

KLHL2 kelch domain (used for crystallography, assays)
Human KLHL2 kelch domain (a.a. 294–593) was cloned into pNIC28-Bsa4, expressed in BL21(DE3)-R3-pRARE cells and purified using Ni-affinity, ion exchange and size exclusion chromatography.

WNK3 kinase domain diphosphorylated (used for crystallography, assays)
Human WNK3 kinase domain (a.a. 133-414) was cloned into pNIC28-Bsa4, expressed in BL21(DE3)-R3-pRARE cells and purified sequentially using Ni-affinity and size-exclusion chromatography. Bacterial expression yielded diphosphorylated WNK3 protein (Ser304 and Ser308). When desired the non-phosphorylated kinase domain was prepared by *in vitro* lambda phosphatase treatment or by bacterial coexpression with lambda phosphatase.

WNK3 kinase domain monophosphorylated (used for crystallography, assays)
Human WNK3 kinase domain (a.a. 132-414) was cloned into pFB-LIC-Bse and prepared by baculoviral expression. Predominantly Ser304 monophosphorylated WNK3 protein was purified sequentially using Ni-affinity and size-exclusion chromatography.

WNK3 kinase-CCT1 domain fusion (used for crystallography, assays)
Human WNK3 kinase and CCT1 domain (a.a. 123-500) were cloned into pFB-LIC-Bse and prepared by baculoviral expression. WNK3 protein was purified sequentially using Ni-affinity and size-exclusion chromatography. When required dephosphorylated WNK3 was prepared by co-infection of baculovirus expressing lambda phosphatase.

WNK3 CCT1 domain (used for assays)
Human WNK3 CCT1 domain (a.a. 406-500) was cloned into pNIC28-Bsa4, expressed in *E. coli* strain BL21(DE3)-R3-pRARE cells and purified sequentially using Ni-affinity and size-exclusion chromatography.

WNK3 CCT2 domain (used for assays)
Human WNK3 CCT2 domain (a.a. 741-820) was cloned into pNIC28-Bsa4, expressed in *E. coli* strain BL21(DE3)-R3-pRARE cells and purified sequentially using Ni-affinity and size-exclusion chromatography.

WNK1 CCT1 domain (used for assays)
Human WNK1 CCT1 domain (a.a. 480-572) was cloned into pNIC28-Bsa4, expressed in *E. coli* strain BL21(DE3)-R3-pRARE cells and purified sequentially using Ni-affinity and size-exclusion chromatography.

WNK1 CCT2 domain (used for crystallography and assays)
Human WNK1 CCT2 domain (a.a. 1115-1194) was cloned into pNIC28-Bsa4, expressed in *E. coli* strain BL21(DE3)-R3-pRARE cells and purified sequentially using Ni-affinity and size-exclusion chromatography.

WNK4 CCT2 domain (used for assays)
Human WNK4 CCT2 domain (a.a. 671-751) was cloned into pNIC28-Bsa4, expressed in *E. coli* strain BL21(DE3)-R3-pRARE cells and purified sequentially using Ni-affinity and size-exclusion chromatography.

SPAK CCT domain (used for assays)
Human SPAK CCT domain (a.a. 448-547) was cloned into pNIC28-Bsa4, expressed in *E. coli* strain BL21(DE3)-R3-pRARE cells and purified sequentially using Ni-affinity and size-exclusion chromatography.

OSR1 CCT domain (used for assays)
Human OSR1 CCT domain (a.a. 432-527) was cloned into pNIC28-Bsa4, expressed in *E. coli* strain BL21(DE3)-R3-pRARE cells and purified sequentially using Ni-affinity and size-exclusion chromatography.

Structural data

1. WNK1 CCT2 domain (1.6 Å, PDB 5G3Q)
2. WNK3 degron peptide + KLHL3 kelch domain (2.8 Å, PDB 5NKP)
3. WNK4 degron peptide + KLHL2 kelch domain (1.6 Å, PDB 4CHB)
4. WNK4 degron peptide + KLHL3 kelch domain (1.8 Å, PDB 4CH9)
5. WNK3 kinase monophosphorylated apo (2.7 Å, PDB 5O23)
6. WNK3 kinase A-loop exchange (1.7 Å, PDB 5O1V)
7. WNK3 kinase + inhibitory Cl^- ion (2.0 Å, PDB 5O21)
8. WNK3 kinase diphosphorylated + AMP-PNP, (2.4 Å, PDB 5O26)
9. WNK3 kinase + PP121 inhibitor (2.0 Å, PDB 5O2B)
10. WNK3 kinase-CCT1 fusion (2.4 Å, PDB 5O2C)

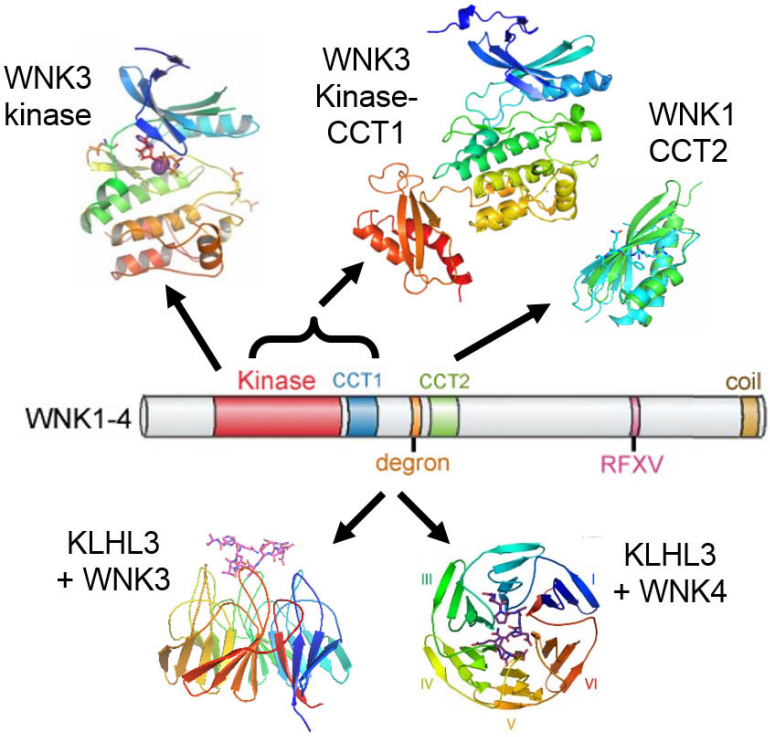

Fig.3. Overview highlighting the diversity of WNK-family crystal structures determined in this study

Structural rationale for Gordon's syndrome mutations

The WNK1-4 acidic degron motif binds to the KLHL2 and KLHL3 kelch domains in a manner distinct to the KEAP1 kelch domain consistent with their binding selectivity (**Fig. 4**).

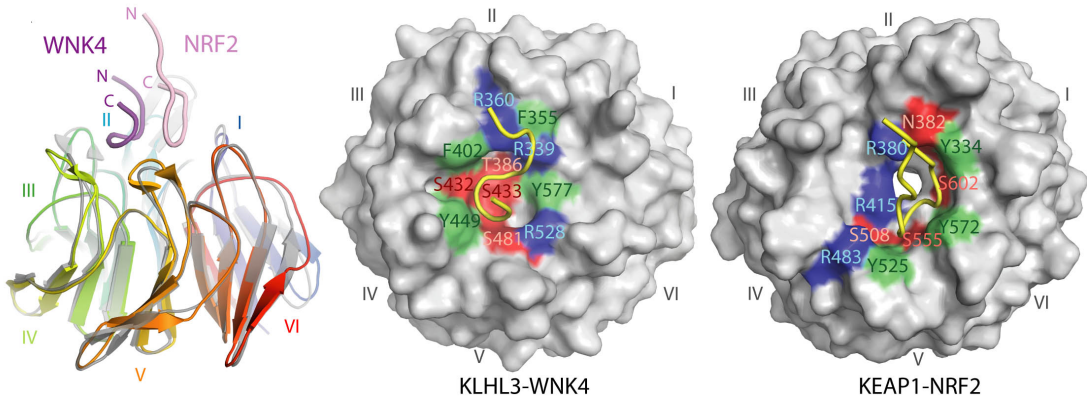

Fig. 4. Comparison of KLHL3-WNK4 and KEAP1-Nrf2 complexes

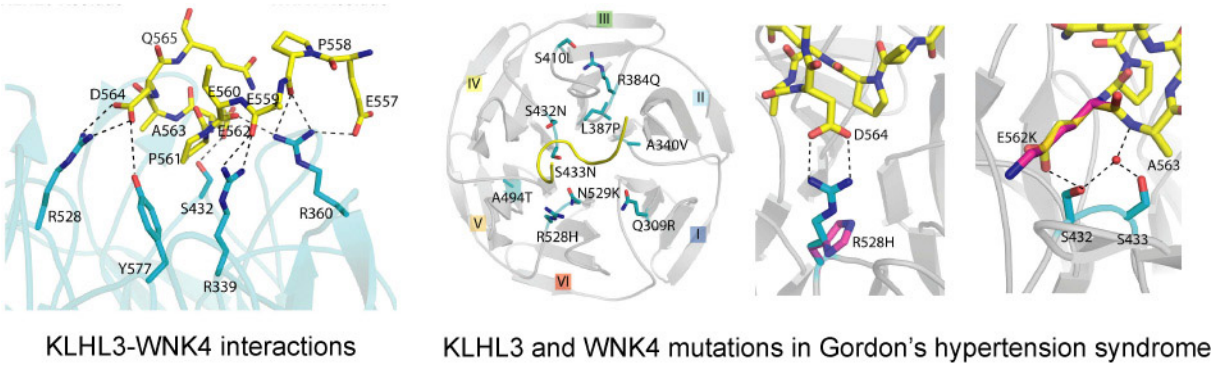

Fig. 5. Structural basis for KLHL3 and WNK4 mutations in hypertension

Analysis of the KLHL3-WNK4 interface shows that many of the disease-causing mutations inhibit binding by disrupting critical interface contacts (e.g. **Fig. 5**; KLHL3 R528H and WNK4 E562K). Others are predicted to have a negative impact on the overall tertiary structure and stability of the KLHL3 protein. Loss of WNK4 binding to the KLHL3 E3 ligase prevents its ubiquitination and therefore results in WNK4 stabilisation and a gain of function. The structure of the more divergent WNK3 degron in complex with KLHL3 shows that all WNK isoforms bind similarly to KLHL2 and KLHL3 kelch domains. Further description of the interfaces can be found in Biochem J. (2014) 460, 237–246.

Structural insights into the WNK3 kinase domain

The apo and chloride-bound structures of the WNK3 kinase domain exhibit an inactive kinase conformation characterised by an αC-out conformation and an inhibitory αAL helix formed within the activation loop that supports the inhibitory function of chloride ions. By contrast, the inhibitory αAL helix was lost in WNK3 complexes with AMP-PNP or the inhibitor PP121. Surprisingly, these complexes retained an αC-out conformation despite the presence of activation loop phosphorylation on WNK3 Ser304 and Ser308 (Fig. 6). This suggests that other as yet unknown factors may also regulate formation of the active WNK kinase conformation.

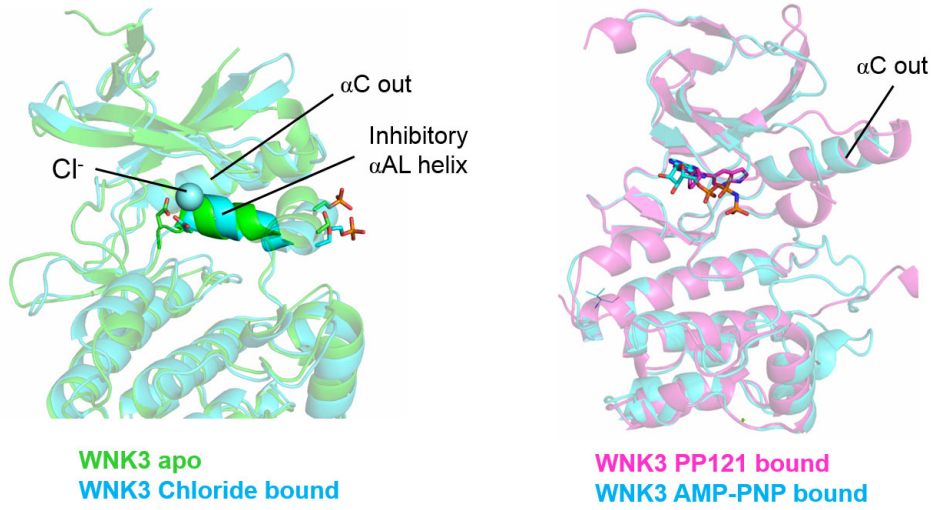

Fig. 6. Kinase structural changes upon ligand binding

Structural insights into the CCT1 and CCT2 domains

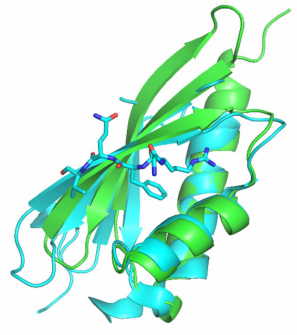

WNK1 CCT2 domain
OSR1 CCT domain with
WNK4 RFXV peptide (PDB 2V3S)

Fig.7. First structure of the hypothetical CCT2 domain highlighting its similarity to a OSR1 CCT domain-RFXV peptide complex.

Interactions in the cascade between WNKs, SPAK/OSR1 and co-transporters are facilitated by RFXV peptide motif interactions with Conserved C-Terminal (CCT) domains in the kinases SPAK, OSR1 and WNK1-4. We determined the first structure of a WNK3 CCT1 domain attached to the kinase domain showing its proximity to the kinase active site (**Fig. 3**). We also prepared the first protein for the predicted WNK CCT2 regulatory domain and were able to solve the crystal structure of the WNK1 CCT2 domain (**Fig. 7**). This structure shows that the hypothetical CCT2 domain is indeed folded similarly to other known CCT domains.

Structural insights into the binding of WNK3 kinase inhibitors

The WNK3 kinase domain was solved in complex with the type I inhibitor PP121. The complex shows a DLG-in, αC-out conformation that creates an allosteric pocket that can be exploited for inhibitor development (**Fig. 8**). Concurrently, with this work this concept was demonstrated independently by Novartis who published their inhibitor WNK463 bound to a similar pocket in WNK1 (PDB 5DRB; (4)).

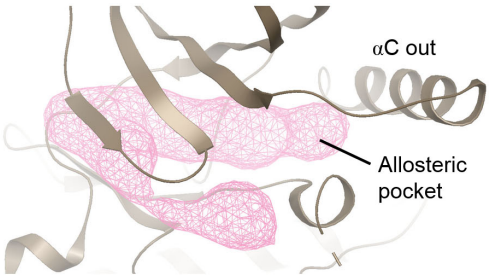

WNK3 analysis by ICM Pocket Finder

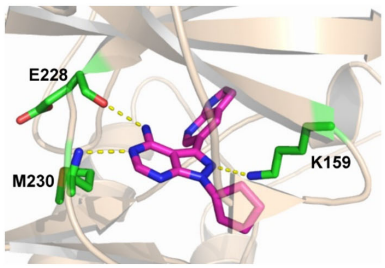

WNK3 complex with inhibitor PP121

Fig. 8. PP121 inhibitor binding to WNK3

In vitro assays

1. Fluorescence polarisation assay for WNK degron binding to KLHL2/3 kelch domains
2. Fluorescence polarisation assay for CCT domain-RFXV peptide interaction
3. Thermal shift assay as an initial inhibitor binding screen
4. In vitro kinase assays

FP assay of WNK degron capture by KLHL3

A fluorescence polarisation (FP) assay was used to measure the binding of WNK degron motif-containing peptides to the kelch domains of KLHL2 and KLHL3. Binding was in the low micromolar range for both KLHL2 and KLHL3, except for WNK4 peptides containing disease-associated mutations which caused a dramatic reduction in binding (**Fig. 9**)(5).

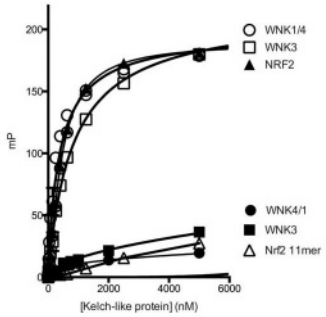

KLHL3 (open) and KEAP1 (solid) binding to different WNK and Nrf2 peptides

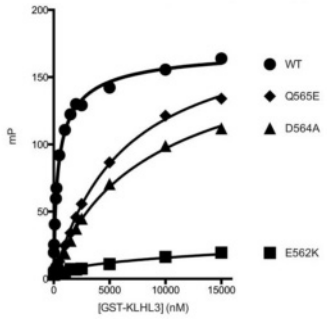

Reduced binding of KLHL3 to WNK4 mutants

Peptide	K_D (μM)
WNK1/4	0.35
WNK3	0.84
WNK4 Q565E	6.2
WNK4 D564A	poor binding
WNK4 E562K	poor binding

Fig. 9. FP assay for WNK degron binding to KLHL3

Inhibitor binding assays

Prior to this study there was little evidence for WNK kinase inhibitors, except for one screen in 2009 reporting WNK1 inhibition by Src-family inhibitors PP1 and PP2 (PP1 Ki = 12.7 μM; (6)). We used a fluorescence-based thermal shift assay (differential scanning fluorimetry, DSF) to screen a collection of 860 kinase inhibitors obtained from commercial vendors or GSK's PKIS inhibitor set (7). Remarkably, only 3 compounds produced a thermal shift of >3°C suggesting that the atypical β2 lysine in WNK kinases may interfere with the binding of many known traditional inhibitors (Fig. 11). The top hit (ΔT_m > 5.7°C) was the inhibitor PP121 developed by Kevan Shokat (8). A radiolabelled *in vitro* kinase assay showed that PP121 inhibited WNK1 and WNK3 with IC50 values of 160 nM and 215 nM, respectively.

Chemical starting points

Chemical matter with co-structures included AMP-PNP as well as PP121, which was developed as a dual inhibitor of tyrosine kinases and phosphatidylinositol-3-OH kinases (8).

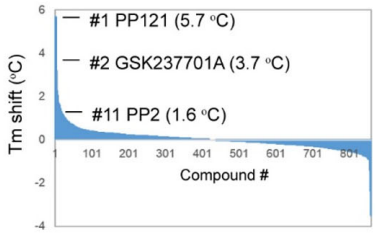

Thermal shift assay using WNK3 identifies PP121

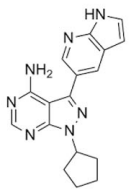

PP121

WNK1 IC_{50} = 160 nM
WNK3 IC_{50} = 215 nM
Ligand Efficiency = 0.39
Ligand-lipophilicity Efficiency = 4.0

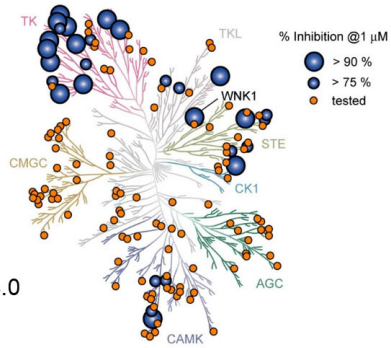

Kinase selectivity profile for PP121 (144 kinases, MRC PPU, Dundee)

Fig. 11. Identification of PP121 as a WNK3 inhibitor

IMPORTANT: Please note that the existence of small molecules within this TEP indicates that chemical matter can bind to the protein in a functionally relevant pocket. As such these molecules should not be used as tools for functional studies of the protein unless otherwise stated as they are not sufficiently potent or well-characterised to be used in cellular studies. The small molecule ligands are intended to be used as the basis for future chemistry optimisation to increase potency and selectivity and yield a chemical probe or lead series.

Antibodies

The following sheep polyclonal antibody has proved effective: WNK3 1142-1461 [DU 4933; sheep S156C] available from MRC PPU Reagents and Services, University of Dundee.

CRISPR/Cas9 Reagents

Reagents targeting human WNK3 have been published by others in Nat Biotech (2016) 34, 184–191 and are available from Addgene (plasmids #76925, #76926, #76927). Alternatively, reagents are available from the human Dharmacon SMARTpool siRNA kinome library.

Future questions

- Further optimisation of chemical matter
- Further exploration of WNK3 as a therapeutic target in hypertension and stroke
- Further characterisation of WNK3 kinase activation

Collaborations

- WNK3 functional assays: Dario Alessi, MRC PPU, University of Dundee

CONCLUSION

WNK kinases control blood pressure and cell volume via their regulation of cation-chloride cotransporters. Genetic evidence supports their potential value as therapeutic targets in hypertension as well as for neuroprotection after stroke. We show that hypertension-associated mutations disrupt the recruitment of WNK kinases to the E3 ligases KLHL2 and KLHL3. This TEP additionally provides a wealth of structural data to support further functional studies and inhibitor development, including the first structure of a WNK-CCT1 domain construct and the first structure of the predicted CCT2 domain.

PP121 was identified as one of the very few inhibitors apparently compatible with the atypical ATP-binding pocket of WNK3. The co-crystal structure of WNK3 and PP121 showed an inactive DLG-in, αC-out conformation of the kinase domain offering a potential allosteric pocket for inhibitor design. Indeed, upon completion of this work, Novartis published the compound WNK463 as a pan-WNK kinase inhibitor exploiting this allosteric binding mode (4).

FUNDING INFORMATION

The work performed at the SGC has been funded by a grant from the Wellcome [106169/ZZ14/Z].

ADDITIONAL INFORMATION

Structure Files

PDB ID	Structure Details
5G3Q	WNK1 CCT2 domain
5NKP	WNK3 degron peptide + KLHL3 kelch domain
4CHB	WNK4 degron peptide + KLHL2 kelch domain
4CH9	WNK4 degron peptide + KLHL3 kelch domain
5O23	WNK3 kinase monophosphorylated apo
5O1V	WNK3 kinase A-loop exchange
5O21	WNK3 kinase + inhibitory Cl^- ion
5O26	WNK3 kinase diphosphorylated + AMP-PNP
5O2B	WNK3 kinase + PP121 inhibitor
5O2C	WNK3 kinase-CCT1 fusion

Materials and Methods

Assays

Thermal Shift (DSF) Assay

A fluorescence-based thermal shift assay (DSF) was performed as a screen to identify potential WNK3 inhibitors. Ligands in this assay increase a protein's melting temperature (T_m shift) by an amount proportional to their binding affinity. A solution of 1-2 μM WNK3-CCT1 protein in assay buffer (10 mM HEPES pH 7.5, 150 mM NaCl) was mixed 1:1000 with SYPRO Orange (Invitrogen). Compounds to be tested were added to a final concentration of 12.5 μM. 20 μL of each sample were placed in a 96-well plate and heated from 25 to 95°C. Fluorescence was monitored using a Mx3005P real-time PCR instrument (Agilent) with excitation and emission filters set to 465 and 590 nm, respectively. Data were analysed with the MxPro software and curves fit in Microsoft Excel using the Boltzmann equation to determine the midpoint of thermal denaturation (T_m). Thermal shift values (ΔT_m) induced by inhibitor binding were calculated relative to control wells containing protein and 2.5% DMSO.

In vitro *Kinase Assay*

General protocol: Test samples in 96 well plates are set up containing 0.5 μL inhibitor, 15 μL enzyme, substrate and buffer and incubated at room temperature for 5 min. The assay is initiated by the addition of 10 μL ^{33}P Mg-ATP (at approximately Km for ATP) and incubated at room temperature for 30 min. The assay is then stopped by the addition of orthophosphoric acid, harvested onto P81 filterplates, dried and read on a scintillation counter for 30 sec per well. The assays are published in Biochem J. (2003) 371, 199-204 and Biochem J (2007) 408, 297-315.

WNK3 specific protocol: WNK3 (5-20 mU diluted in 20 mM MOPS pH 7, 1 mM EGTA, 0.01% Brij35, 5% glycerol, 1 mg/mL BSA, 0.1% mercaptoethanol) is assayed against myelin basic protein, MBP, in a final volume of 25.5 μL containing 8 mM MOPS pH 7, 0.02 mM EDTA, 5 mM $MnCl_2$, 0.33 mg/mL MBP, 10 mM magnesium acetate and 0.005 mM [33P-γ-ATP] (50-1000 cpm/pmole) and incubated for 30 min at room temperature. Assays are stopped by addition of 5 μL of 0.5 M (3%) orthophosphoric acid and then harvested onto P81 Unifilter plates with a wash buffer of 50 mM orthophosphoric acid.

Mass spectrometry

Protein masses were determined using an Agilent LC/MSD TOF system with reversed-phase high-performance liquid chromatography coupled to electrospray ionization and an orthogonal time-of-flight mass analyser. Proteins were desalted prior to mass spectrometry by rapid elution off a C3 column with a gradient of 5-95% isopropanol in water with 0.1% formic acid. Spectra were analysed using the MassHunter software (Agilent).

Fluorescence polarisation assay for WNK degron binding to KLHL2/3 kelch domains

Fluorescence polarisation measurements were performed at 25°C with purified KLHL3 proteins in 50 mM Tris-HCl pH 7.5, 150 mM NaCl, 2 mM DTT. All peptides contained an N-terminal linker required for conjugating

to the Lumio green flurophore (CCPGCCGGGG) and were initially resuspended in 50 mM ammonium biocarbonate pH 8. Peptide labelling was achieved by incubating 10 nM of each peptide in a 0.5 mL reaction mixture of 20 μM Lumio green in 50 mM TrisHCl pH 7.5, 150 mM NaCl, 2 mM DTT. Reactions were left to proceed in the dark for 2 h. The peptides were then dialysed for 16 h into 50 mM Tris-HCl pH 7.5, 150 mM NaCl, 2 mM DTT using a Micro DispoDIALYZER with a 100 Da molecular weight cut off (Harvard Apparatus). For fluorescence polarisation, mixtures were set up containing the indicated concentration of protein, 10 nM Lumio-green labelled peptide in a final volume of 30 μL. All individual bindings were performed in duplicate with at least 12 data points per curve. Fluorescence polarisation measures were made using a BMG PheraStar plate reader, with an excitation wavelength of 485 nm and an emission wavelength of 538 nm, and measurements were corrected to the fluorescent probe alone. Data analysis and graphing were then performed in GraphPad Prism; One Site Specific binding with Hill Slope was assumed (model $Y=B_{max}*X\text{^}h/K_d\text{^}h + X\text{^}h$) and the disassociation constant, and associated standard error were obtained. All experimental bindings were repeated a minimum of two times and comparable results were obtained.

Protein Expression and Purification

Human KLHL3 kelch domain
Boundaries: residues 298–587
Vector: pNIC28-Bsa4
Tag and additions: TEV-cleavable N-terminal hexahistidine tag
Expression cell: *E. coli* BL21(DE3)R3-pRARE2

Human KLHL3 kelch domain was expressed from the vector pNIC28-Bsa4 in BL21(DE3)-R3-pRARE cells (a phage-resistant derivative of Rosetta2, Novagen). Cultures (1 litre) in Terrific broth were incubated at 37°C until OD600 reached 2.0 and then cooled to 18°C and supplemented with 0.5 mM IPTG to induce protein expression overnight. Cells were harvested by centrifugation, resuspended in binding buffer (50 mM HEPES pH 7.5, 500 mM NaCl, 5 mM imidazole, 5% glycerol and 0.5 mM TCEP [tris-(2-carboxyethyl)phosphine] and lysed by sonication. The His6-tagged protein was purified using Ni^{2+}-Sepharose resin (GE Healthcare) and eluted stepwise in binding
buffer with 100-250 mM imidazole. Removal of the His6 tag was performed at 4°C overnight using TEV protease. KLHL3 was then further purified by anion exchange chromatography using a 5 mL HiTrap Q column (GE Healthcare) followed by a final buffer-exchange step into 50 mM HEPES pH 7.5, 300 mM NaCl, 5% glycerol and 0.5 mM TCEP using size-exclusion chromatography (Superdex 200 16/60, GE Healthcare).

Human KLHL2 kelch domain
Boundaries: residues 294–593
Vector: pNIC28-Bsa4
Tag and additions: TEV-cleavable N-terminal hexahistidine tag
Expression cell: *E. coli* BL21(DE3)R3-pRARE2

Human KLHL2 kelch domain was expressed from the vector pNIC28-Bsa4 in BL21(DE3)-R3-pRARE cells (a phage-resistant derivative of Rosetta2, Novagen). Cultures (1 litre) in Terrific broth were incubated at 37°C until OD600 reached 2.0 and then cooled to 18°C and supplemented with 0.5 mM IPTG to induce protein expression overnight. Cells were harvested by centrifugation, resuspended in binding buffer (50 mM HEPES pH 7.5, 500 mM NaCl, 5 mM imidazole, 5% glycerol and 0.5 mM TCEP [tris-(2-carboxyethyl)phosphine] and lysed by sonication. The His6-tagged protein was purified using Ni^{2+}-Sepharose resin (GE Healthcare) and eluted stepwise in binding
buffer with 100-250 mM imidazole. Removal of the His6 tag was performed at 4°C overnight using TEV protease. KLHL2 was then further purified by cation exchange chromatography using a 5 mL HiTrap SP column (GE Healthcare) followed by a buffer-exchange step into 50 mM HEPES pH 7.5, 300 mM NaCl, 5% glycerol and 0.5 mM TCEP using size-exclusion chromatography (Superdex 200 16/60, GE Healthcare).

Human WNK3 kinase domain (diphosphorylated)
Boundaries: residues 133–414
Vector: pNIC28-Bsa4
Tag and additions: TEV-cleavable N-terminal hexahistidine tag
Expression cell: *E. coli* BL21(DE3)R3-pRARE2

Human WNK3 kinase domain was expressed from the vector pNIC28-Bsa4 in BL21(DE3)-R3-pRARE cells. Cultures were grown at 37°C in LB medium supplemented with 50 µg/mL kanamycin and 34 µg/mL chloramphenicol to an OD600 of 0.6, before expression at 18°C overnight and induction with 0.3 mM isopropyl 1-thio-β-D-galactopyranoside (IPTG). Cells were then harvested by centrifugation at 5000g and resuspended in binding buffer (50 mM HEPES pH 7.5, 500 mM NaCl, 5% glycerol, 5 mM imidazole, EDTA-free complete protease inhibitor cocktail (Roche)) and lysed by sonication. Lysates were clarified by centrifugation in a JA 25.50 rotor at 36000 g. His-tagged protein was immobilized on Ni^{2+}-sepharose resin and bound proteins eluted using step gradients of Imidazole (50-250 mM). The eluted proteins were cleaved with TEV protease overnight at 4°C and further purified by size exclusion chromatography using an S200 HiLoad 16/60 Superdex column equilibrated in buffer containing 50 mM HEPES pH 7.5, 300 mM NaCl, and 0.5 mM TCEP. Proteins were concentrated using centrifugal ultrafiltration with a 10 kDa molecular weight cut-off point membrane. Protein purity of >95% was confirmed by SDS-PAGE and identity plus phosphorylation state verified by intact mass spectrometry. Bacterial expression yielded diphosphorylated WNK3 protein (Ser304 and Ser308). When desired the non-phosphorylated kinase domain was prepared by in vitro lambda phosphatase treatment or by bacterial coexpression with lambda phosphatase.

Human WNK3 kinase domain (monophosphorylated)
Boundaries: residues 132–414
Vector: pFB-LIC-Bse
Tag and additions: TEV-cleavable N-terminal hexahistidine tag
Expression cell: Sf9 insect cells

Bacmid DNA was prepared from DH10Bac cells and used to transfect Sf9 insect cells for the preparation of initial baculovirus. WNK3 protein was expressed from infected Sf9 cells cultivated in InsectXpress medium (Lonza) for 48 hours at 27°C. Harvested cells were resuspended and purified similarly to the bacterially-expressed WNK3 kinase domain described above. Baculoviral expression resulted in predominantly Ser304 monophosphorylated WNK3 protein.

Human WNK3 kinase-CCT1 domain fusion
Boundaries: residues 123–500
Vector: pFB-LIC-Bse
Tag and additions: TEV-cleavable N-terminal hexahistidine tag
Expression cell: Sf9 insect cells

Bacmid DNA was prepared from DH10Bac cells and used to transfect Sf9 insect cells for the preparation of initial baculovirus. WNK3 protein was expressed from infected Sf9 cells cultivated in InsectXpress medium (Lonza) for 48 hours at 27°C. Harvested cells were resuspended and purified similarly to the bacterially-expressed WNK3 kinase domain described above. When required dephosphorylated WNK3 was prepared by co-infection of baculovirus expressing lambda phosphatase.

Human WNK3 CCT1 domain
Boundaries: residues 406–500
Vector: pNIC28-Bsa4
Tag and additions: TEV-cleavable N-terminal hexahistidine tag
Expression cell: *E. coli* BL21(DE3)R3-pRARE2

See general protocol for preparation of CCT domains below.

Human WNK3 CCT2 domain
Boundaries: residues 741–820
Vector: pNIC28-Bsa4
Tag and additions: TEV-cleavable N-terminal hexahistidine tag
Expression cell: *E. coli* BL21(DE3)R3-pRARE2

See general protocol for preparation of CCT domains below.

Human WNK1 CCT1 domain
Boundaries: residues 480–572
Vector: pNIC28-Bsa4
Tag and additions: TEV-cleavable N-terminal hexahistidine tag
Expression cell: *E. coli* BL21(DE3)R3-pRARE2

See general protocol for preparation of CCT domains below.

Human WNK1 CCT2 domain
Boundaries: residues 1115–1194
Vector: pNIC28-Bsa4
Tag and additions: TEV-cleavable N-terminal hexahistidine tag
Expression cell: *E. coli* BL21(DE3)R3-pRARE2

See general protocol for preparation of CCT domains below.

Human WNK4 CCT2 domain
Boundaries: residues 671–751
Vector: pNIC28-Bsa4
Tag and additions: TEV-cleavable N-terminal hexahistidine tag
Expression cell: *E. coli* BL21(DE3)R3-pRARE2

See general protocol for preparation of CCT domains below.

Human SPAK CCT domain
Boundaries: residues 448–547
Vector: pNIC28-Bsa4
Tag and additions: TEV-cleavable N-terminal hexahistidine tag
Expression cell: *E. coli* BL21(DE3)R3-pRARE2

See general protocol for preparation of CCT domains below.

Human OSR1 CCT domain
Boundaries: residues 432–527
Vector: pNIC28-Bsa4
Tag and additions: TEV-cleavable N-terminal hexahistidine tag
Expression cell: *E. coli* BL21(DE3)R3-pRARE2

See general protocol for preparation of CCT domains below.

General procedure for CCT domain preparation
Human CCT domains were expressed from the vector pNIC28-Bsa4 in BL21(DE3)-R3-pRARE cells. Cultures were grown at 37°C in LB medium supplemented with 50 µg/mL kanamycin and 34 µg/mL chloramphenicol to an OD600 of 0.6, before expression at 18°C overnight and induction with 0.3 mM isopropyl 1-thio-β-D-galactopyranoside (IPTG). Cells were then harvested by centrifugation at 5000g and resuspended in binding buffer (50 mM HEPES pH 7.5, 500 mM NaCl, 5% glycerol, 5 mM imidazole, EDTA-free complete protease

inhibitor cocktail (Roche)) and lysed by sonication. Lysates were clarified by centrifugation in a JA 25.50 rotor at 36000 g. His-tagged protein was immobilized on Ni^{2+}-sepharose resin and bound proteins eluted using step gradients of Imidazole (50-250 mM). The eluted proteins were cleaved with TEV protease overnight at 4°C and further purified by size exclusion chromatography using an S75 HiLoad 16/60 Superdex column equilibrated in buffer containing 50 mM HEPES pH 7.5, 300 mM NaCl, and 0.5 mM TCEP. Proteins were concentrated using centrifugal ultrafiltration with a 3 kDa molecular weight cut-off point membrane. Protein purity of >95% was confirmed by SDS-PAGE and identity verified by intact mass spectrometry. Protein concentrations were determined by measuring absorbance at 280 nm, or in cases where extinction coefficients were too low, concentrations were determined using Bradford assays and validated with a Direct Detect Infrared Spectrometer.

Structure Determination

KLHL3/WNK4 complex (PDB: 4CH9)

KLHL3 protein was concentrated to 9 mg/mL and mixed with 2 mM final concentration WNK4 peptide (EPEEPEADQHQ) for 30 minutes on ice. Crystallisation was performed using sitting-drop vapour-diffusion. Crystals of the KLHL3 complex were obtained at 20°C by mixing 100 nL of protein with 50 nL of a reservoir solution containing 0.1 M acetate pH 4.3, 0.2 M ammonium sulphate and 25-35 % PEG 4000. After 3 hours of incubation the drops were spiked with 20 nL of seed-stock solution. Prior to vitrification in liquid nitrogen, crystals were cryoprotected by direct addition of reservoir solution supplemented with 25 % ethylene glycol. Diffraction data were collected on beamline I02 at Diamond Light Source. Diffraction data were integrated using Mosflm and scaled using SCALA from the CCP4 software suite. Molecular replacement was performed with Phaser MR in CCP4 using PDB ID code 2XN4 chain A (apo kelch domain of KLHL2) as the search model. COOT was used for manual model building and refinement, while REFMAC and PHENIX.REFINE were used for automated refinement. TLS parameters were included at later stages of refinement. Tools in COOT, PHENIX and MolProbity were used to validate the structures.

KLHL2/WNK4 complex (PDB: 4CHB)

KLHL2 protein was concentrated to 9 mg/mL and mixed with 2 mM final concentration WNK4 peptide (EPEEPEADQHQ). The protein-peptide solution was incubated on ice for approximately 30 minutes prior to preparation of sitting-drop vapour-diffusion crystallisation plates. Diffracting crystals were obtained at 20°C by mixing 100 nL of protein with 50 nL of a reservoir solution containing 0.1 M HEPES pH 7.2, 2.5 M ammonium sulphate and 2 % PEG 400. After 3 hours of incubation the drops were spiked with 20 nL of seed-stock solution. Prior to vitrification in liquid nitrogen, crystals were cryoprotected by direct addition of reservoir solution supplemented with 25 % ethylene glycol. Diffraction data were collected on beamline I02 at Diamond Light Source. Diffraction data were integrated using Mosflm and scaled using SCALA from the CCP4 software suite. Molecular replacement was performed with Phaser MR in CCP4 using PDB ID code 2XN4 chain A (apo kelch domain of KLHL2) as the search model. COOT was used for manual model building and refinement, while REFMAC and PHENIX.REFINE were used for automated refinement. TLS parameters were included at later stages of refinement. Tools in COOT, PHENIX and MolProbity were used to validate the structures.

KLHL3/WNK3 complex (PDB: 5NKP)

KLHL3 was concentrated to 9 mg/mL buffered in 50 mM HEPES pH 7.5, 300 mM NaCl, 0.5 mM TCEP, 2 mM DTT and mixed with 2 mM WNK3 acidic motif peptide (ECEETEVDQHV). Diffracting crystals were obtained at 4°C in sitting drops by mixing 100 nL protein with 50 nL solution containing 6% PEG4K, 0.1 M acetate pH 5.1. After 3 hours of incubation the drops were spiked with 20 nL of seed-stock solution. Prior to vitrification in liquid nitrogen, crystals were cryoprotected by direct addition of reservoir solution supplemented with 25 % ethylene glycol. Diffraction data were collected on beamline I03 at Diamond Light Source. Diffraction data were processed using PHENIX. Molecular replacement was performed with Phaser MR in Phenix using PDB 4CH9 as the model. COOT was used for manual model building and refinement, whereas PHENIX.REFINE was used for automated refinement. TLS parameters were included at later stages of refinement.

General methods for structure determination of WNK kinase and CCT domains

Data were indexed and integrated using XDS and scaled using AIMLESS in the CCP4 suite of programs. Phases were found using molecular replacement in PHASER. Models were built initially using COOT and then refined and modified using alternate rounds of REFMAC5 and COOT. Specific details for each structure are listed below.

WNK3 kinase-CCT1 (dephosphorylated)

Dephosphorylated WNK3 Kinase-CCT1 (a.a. 123-500) was buffered in 50 mM HEPES pH 7.5, 300 mM NaCl, 5% glycerol, 0.5 mM TCEP, and concentrated to 9.6 mg/mL. Crystals were grown at 4°C in 400 nL sitting drops at a 1:1 protein: reservoir solution comprising 18% PEG3350, 0.1 M citrate pH 5. Before mounting, crystals were cryo-protected with mother liquor supplemented with an additional 25 % glycerol and vitrified in liquid nitrogen. Diffraction data were collected at Diamond Light Source beamline I03.

WNK3 kinase domain (apo, monophosphorylated)

Monophosphorylated WNK3 kinase domain (a.a. 132-414) was buffered in 50 mM HEPES pH 7.5, 300 mM NaCl, 0.5 mM TCEP, and concentrated to 12.3 mg/mL. Crystals were grown at 20°C in 150 nL sitting drops at a 1:1 protein: reservoir solution comprising 30% PEG Smear Medium, 0.2 M lithium sulfate, 0.1 M ADA pH 6.5. Before mounting, crystals were cryo-protected with mother liquor supplemented with an additional 25% ethylene glycol and vitrified in liquid nitrogen. Diffraction data were collected at Diamond Light Source beamline I03.

WNK3 kinase (Cl^- bound, monophosphorylated)

Monophosphorylated WNK3 kinase domain (a.a. 132-414) was buffered in 50 mM HEPES pH 7.5, 300 mM NaCl, 0.5 mM TCEP, and concentrated to 10 mg/mL. 1 mM adenosine diphosphate (ADP) and 2 mM $MgCl_2$ were added, but not observed in the resulting structure. Crystals were grown at 4°C in 150 nL sitting drops at a 2:1 protein: reservoir solution comprising 22.5% PEG Smear Broad, 0.1 M sodium/potassium tartrate, 10% ethylene glycol, 0.1 M cacodylate pH 5.5. Before mounting, crystals were cryo-protected with mother liquor supplemented with an additional 25 % ethylene glycol and vitrified in liquid nitrogen. Anomalous data with high redundancy were collected at Diamond Light Source beamline I04 using a wavelength of 1.77Å.

WNK3 kinase (monophosphorylated, A-loop exchange)

Monophosphorylated WNK3 kinase domain (a.a. 132-414) was buffered in 50 mM HEPES pH 7.5, 300 mM NaCl, 0.5 mM TCEP, and concentrated to 10 mg/mL. 1 mM adenylyl-imidodiphosphate (AMP-PNP) and 2 mM $MgCl_2$ were added, but not observed in the resulting structure. Crystals were grown at 4°C in 150 nL sitting drops at a 2:1 protein: reservoir solution comprising 20% PEG4000, 10% 2-propanol, 0.1M HEPES pH 7.5. Before mounting, crystals were cryo-protected with mother liquor supplemented with an additional 25 % ethylene glycol and vitrified in liquid nitrogen. Diffraction data were collected at Diamond Light Source beamline I04.

WNK3 kinase (AMP-PNP bound, diphosphorylated)

Diphosphorylated WNK3 kinase domain (a.a 133-414) was buffered in 50 mM HEPES pH 7.5, 50 mM NaCl, 0.5 mM TCEP, 10 mM DTT and concentrated to 9.5 mg/mL. A final concentration of 4 mM adenylyl-imidodiphosphate (AMP-PNP) and 10 mM $MgCl_2$ were added. Crystals were grown at 20°C in 150 nL sitting drops at a 1:2 protein: reservoir solution comprising 25% PEG3350, 0.1M bis-tris pH 5.5. Before mounting, crystals were cryo-protected with mother liquor supplemented with an additional 25 % ethylene glycol and vitrified in liquid nitrogen. Diffraction data were collected at Diamond Light Source beamline I04.

WNK3 kinase (PP121 bound, diphosphorylated)

Diphosphorylated WNK3 kinase domain (a.a 133-414) was buffered in 50 mM HEPES, 50 mM NaCl, 1 mM TCEP and concentrated to 9 mg/mL. A final concentration of 1 mM PP121 was added. Crystals were grown at 20°C in 150 nL sitting drops at a 1:1 protein: reservoir solution comprising 25% PEG3350, 0.2M magnesium chloride, 0.1M bis-tris pH 5.5. Before mounting, crystals were cryo-protected with mother liquor supplemented with an additional 25 % ethylene glycol and vitrified in liquid nitrogen. Diffraction data were collected at Diamond Light Source beamline I04.

WNK1 CCT2 domain

WNK1 CCT2 domain (a.a 1115-1201) was buffered in 20 mM HEPES, 100 mM NaCl and concentrated to 12 mg/mL. Crystals were grown at 20°C in 150 nL sitting drops at a 1:1 protein: reservoir solution comprising 25% PEG3350, 0.2 M ammonium sulfate, 0.1 M bis-tris pH 6.5. Before mounting, crystals were cryo-protected with mother liquor supplemented with an additional 25 % ethylene glycol and vitrified in liquid nitrogen. Diffraction data were collected at Diamond Light Source beamline I04-1.

References

1. Alessi, D. R., Zhang, J., Khanna, A., Hochdorfer, T., Shang, Y., and Kahle, K. T. (2014) The WNK-SPAK/OSR1 pathway: master regulator of cation-chloride cotransporters. *Science signaling* **7**, re3

2. Wu, S., Niu, W., Zhang, Y., Gao, P., and Zhu, D. Gender-specific association between polymorphisms in the WNK3 gene and essential hypertension in a Chinese population. *International Journal of Cardiology* **137**, S111

3. Begum, G., Yuan, H., Kahle, K. T., Li, L., Wang, S., Shi, Y., Shmukler, B. E., Yang, S. S., Lin, S. H., Alper, S. L., and Sun, D. (2015) Inhibition of WNK3 Kinase Signaling Reduces Brain Damage and Accelerates Neurological Recovery After Stroke. *Stroke* **46**, 1956-1965

4. Yamada, K., Park, H. M., Rigel, D. F., DiPetrillo, K., Whalen, E. J., Anisowicz, A., Beil, M., Berstler, J., Brocklehurst, C. E., Burdick, D. A., Caplan, S. L., Capparelli, M. P., Chen, G., Chen, W., Dale, B., Deng, L., Fu, F., Hamamatsu, N., Harasaki, K., Herr, T., Hoffmann, P., Hu, Q. Y., Huang, W. J., Idamakanti, N., Imase, H., Iwaki, Y., Jain, M., Jeyaseelan, J., Kato, M., Kaushik, V. K., Kohls, D., Kunjathoor, V., LaSala, D., Lee, J., Liu, J., Luo, Y., Ma, F., Mo, R., Mowbray, S., Mogi, M., Ossola, F., Pandey, P., Patel, S. J., Raghavan, S., Salem, B., Shanado, Y. H., Trakshel, G. M., Turner, G., Wakai, H., Wang, C., Weldon, S., Wielicki, J. B., Xie, X., Xu, L., Yagi, Y. I., Yasoshima, K., Yin, J., Yowe, D., Zhang, J. H., Zheng, G., and Monovich, L. (2016) Small-molecule WNK inhibition regulates cardiovascular and renal function. *Nature chemical biology* **12**, 896-898

5. Schumacher, F. R., Sorrell, F. J., Alessi, D. R., Bullock, A. N., and Kurz, T. (2014) Structural and biochemical characterization of the KLHL3-WNK kinase interaction important in blood pressure regulation. *The Biochemical journal* **460**, 237-246

6. Yagi, Y. I., Abe, K., Ikebukuro, K., and Sode, K. (2009) Kinetic mechanism and inhibitor characterization of WNK1 kinase. *Biochemistry* **48**, 10255-10266

7. Elkins, J. M., Fedele, V., Szklarz, M., Abdul Azeez, K. R., Salah, E., Mikolajczyk, J., Romanov, S., Sepetov, N., Huang, X.-P., Roth, B. L., Al Haj Zen, A., Fourches, D., Muratov, E., Tropsha, A., Morris, J., Teicher, B. A., Kunkel, M., Polley, E., Lackey, K. E., Atkinson, F. L., Overington, J. P., Bamborough, P., Müller, S., Price, D. J., Willson, T. M., Drewry, D. H., Knapp, S., and Zuercher, W. J. (2015) Comprehensive characterization of the Published Kinase Inhibitor Set. *Nature Biotechnology* **34**, 95

8. Apsel, B., Blair, J. A., Gonzalez, B., Nazif, T. M., Feldman, M. E., Aizenstein, B., Hoffman, R., Williams, R. L., Shokat, K. M., and Knight, Z. A. (2008) Targeted polypharmacology: discovery of dual inhibitors of tyrosine and phosphoinositide kinases. *Nature chemical biology* **4**, 691-699

We respectfully request that this document is cited using the DOI value as given above if the content is used in your work.